Nanoscale Res Lett (2007) 2:297–302
DOI 10.1007/s11671-007-9064-6

NANO EXPRESS

Origin of defect-related green emission from ZnO nanoparticles: effect of surface modification

Yinyan Gong · Tamar Andelman · Gertrude F. Neumark · Stephen O'Brien · Igor L. Kuskovsky

Received: 28 February 2007 / Accepted: 11 May 2007 / Published online: 12 June 2007

Abstract We investigated the optical properties of colloidal-synthesized ZnO spherical nanoparticles prepared from 1-octadecene (OD), a mixture of trioctylamine (TOA) and OD (1:10), and a mixture of trioctylphosphine oxide (TOPO) and OD (1:12). It is found that the green photoluminescence (PL) of samples from the mixture of TOA/OD and TOPO/OD is largely suppressed compared with that from pure OD. Moreover, it is found that all spherical nanoparticles have positive zeta potential, and spherical nanoparticles from TOA/OD and TOPO/OD have a smaller zeta potential than those from OD. A plausible explanation is that oxygen vacancies, presumably located near the surface, contribute to the green PL, and the introduction of TOA and TOPO will reduce the density of oxygen vacancies near the surfaces. Assuming that the green emission arises due to radiative recombination between deep levels formed by oxygen vacancies and free holes, we estimate the size of optically active spherical nanoparticles from the spectral energy of the green luminescence. The results are in good agreement with results from TEM. Since this method is independent of the degree of confinement, it has a great advantage in providing a simple and practical way to estimate the size of spherical nanoparticles of any size. We would like to point out that this method is only applicable for samples with a small size distribution.

Y. Gong (✉) · T. Andelman · G. F. Neumark · S. O'Brien
Department of Applied Physics and Applied Mathematics, Columbia University, New York, NY 10027, USA
e-mail: yg2002@columbia.edu

I. L. Kuskovsky
Department of Physics, Queens College of CUNY, Flushing, NY 11367, USA

Keywords ZnO · Photoluminescence · Nanoparticles · Green emission · Surface modification

Introduction

Zinc oxide (ZnO) is a direct wide band gap semiconductor with an energy gap of ~3.37 eV [1] and a large exciton binding energy of ~60 meV [2] at room temperature (RT). These unique properties make ZnO a promising candidate for applications in optical and optoelectronic devices [3–6]. Furthermore, it is well known that low-dimensional structures may have superior optical properties over bulk material due to the quantum confinement effect (see e.g. Ref. [7]). Lately, there have been extensive studies on the synthesis, electrical, and optical properties of ZnO nanocrystals (see e.g. Refs. [8–11]). A detailed description of the basic properties, applications, and recent advances can be found in Ref. [12].

Typically, the photoluminescence (PL) spectrum of ZnO exhibits a near-band-edge UV emission and a broad defect-related visible emission. This defect-related visible emission is most commonly green luminescence, though other emissions such as yellow or blue have also been observed. For device applications, such as high efficiency UV light emitting devices, it is important to suppress the visible emission. In spite of the numerous studies (see e.g. Refs. [13–20]) on the green luminescence, its origin is still controversial, and a number of suggestions have been proposed. The green luminescence has been attributed to various types of defects such as oxygen vacancies [13–17], zinc vacancies [18], as well as donor–acceptor pairs [19, 20]. To make the situation more complicated, it has been reported that the spectral position and the intensity of the visible emission also depend on the fabrication process (see

e.g. Ref. [21]). A plausible explanation is that the species of impurities as well as the concentration of intrinsic and extrinsic defects are related to the growth procedure. Thus, the dominate defects for the visible emission might be different for samples grown by various techniques, and great care has to be taken when comparing the PL of samples prepared by various growth techniques.

We present here results of PL, optical absorption, and zeta-potential measurements for colloidal-synthesized ZnO spherical nanoparticles prepared from 1-octadecene (OD), a mixture of trioctylamine (TOA) and OD (1:10) as well as a mixture of trioctylphosphine oxide (TOPO) and OD (1:12) with an aim to modify surface states. The synthesis method has been previously reported for ZnO quantum rods [22] (diameter, D = 2.2 nm) as well as for nanocrystals of various morphologies [23].

A strong near-band-edge UV luminescence was observed for all samples: the maximum of the UV PL is approximately at the same spectral position, whereas its spectral width varies. No specific reason for such behavior can be found at the present time. In addition, a weak broad green band was observed. It is found that the green PL of samples prepared from the mixture of TOA/OD and TOPO/OD is effectively quenched compared with that from pure OD. A plausible explanation is that oxygen vacancies, presumably located near the surface, contribute to the green PL and the introduction of TOA and TOPO will reduce oxygen vacancies near the surfaces.

Assuming that the green emission arises due to radiative recombination between deep levels and free holes (see below), we estimate the size of optically active spherical nanoparticles from the energy of the green luminescence. The estimated sizes are in good agreement with results from TEM observations. It is important to note that compared with the calculations that use the exciton ground state energy, this approach does not have limitation on the degree of confinement. Thus, it provides an easy, fast, and sufficiently accurate way to estimate sizes of spherical nanoparticles based on optical measurements.

Experimental

In the standard synthesis, the precursor ($ZnAc_2{\cdot}2H_2O$) and capping agent (oleic acid) are mixed in a 1:1 ratio in OD, which is referred to as the regular solvent, and then heated to 290 °C until the solution turns cloudy/white, indicating the growth of ZnO spherical nanoparticles [23]. Details of the synthesis procedure have been given in Ref. [23]. The size of the ZnO nanoparticles is controlled by the reaction time. To investigate the origin of the commonly observed green emission, we also prepared ZnO spherical nanoparticles from: 1) the mixture of TOA and OD in a 1:10 molar ratio; 2) the mixture of TOPO and OD in a 1:12 molar ratio. It is expected that samples from TOA/OD and TOPO/OD will have modified surface states compared with that from pure OD.

ZnO spherical nanoparticles were characterized by high resolution transmission electron microscopy (JEOL 100cx). For TEM measurements, a drop of nanoparticle solution was placed on a 400 mesh carbon grid with Formvar. The PL measurements were performed at RT using the 325 nm emission from a He–Cd laser. The PL was dispersed through a 3/4 m monochromator, and was detected with a thermoelectrically cooled GaAs photomultiplier tube coupled to a SR400 photon counter. In addition, RT UV-visible absorption spectra were recorded with an Agilent HP8453 spectrometer. Finally, the zeta potential of the spherical nanoparticles from different solvents was measured by Malvern Zetasizer Nano-ZS test measurement system. For all optical as well as mobility measurements nanocrystals were isolated from their growth solution and then redispersed in hexane.

Results and Discussion

Figure 1a–c show the TEM images of the ZnO spherical nanoparticles from different solvents. The measured mean diameter is about 5.0 ± 0.4, 4.0 ±0.5, and 5.0 ± 0.8 nm for samples prepared from OD, the mixture of TOA/OD (1:10), and the mixture of TOPO/OD (1:12), respectively. The spherical nanoparticles from OD with longer reaction time have a diameter ranging from 12 to 14 nm [23].

Figure 2 shows the RT PL of ZnO spherical nanoparticles prepared from pure OD with different diameters. As a reference, we plot PL of a free standing bulk ZnO sample provided by Dr. Rojo of SUNY Stony Brook (curve c). It was found that the PL from all three samples is dominated by the near-band-edge UV emission, and the defect-related green luminescence is only observed for the small spherical nanoparticles. This implies that the green luminescence is associated with defects near the surface, and thus it is quenched with the increasing of the diameters. This is consistent with previous studies on ZnO nanocrystals with different surface-to-volume ratios [23–29]. For example, it has been reported [29] that the visible emission from nanowires decreases as the wire diameter increases. Moreover, previously we found that [23] green luminescence from ZnO nanocrystals with different morphologies is quenched with the decreasing of the surface-to-volume ratio.

Next, to gain insight on the chemical identity of the defects, we compared the PL from ZnO spherical nanoparticles prepared from different solvents (we would like to point out that all spherical nanoparticles are of a compa-

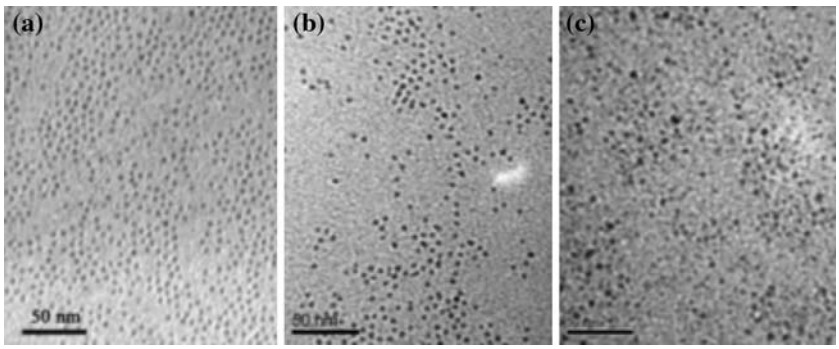

Fig. 1 TEM images of small spherical nanoparticles prepared from (**a**) the regular solvent OD; (**b**) the mixture of TOA and OD in 1:10 molar ratio; (**c**) the mixture of TOPO and OD in 1:12 molar ratio

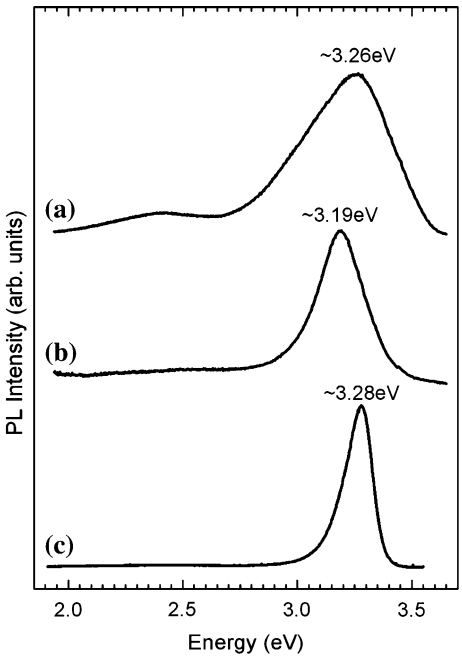

Fig. 2 Room temperature photoluminescence spectra of ZnO (**a**) small spherical nanoparticles with ~5 nm in diameter; (**b**) large spherical nanoparticles with ~12–14 nm in diameter; (**c**) bulk ZnO

rable size, as confirmed by TEM observations). In Fig. 3a–c we show RT PL (black circles) and absorption (inset) spectra of ZnO nanoparticles prepared from: (a) the regular solvent, OD; b) the mixture of TOA and OD in a 1:10 molar ratio; c) the mixture of TOPO and OD in a 1:12 molar ratio. The absorption spectra of all samples exhibit an excitonic absorption peak at ~3.46, ~3.46, and ~3.42 eV, respectively. The PL of all samples is dominated by the near-band-edge UV emission, which is accompanied by a weak broad green band. The relative intensity of the green and UV PL (I_{green}/I_{UV}) strongly depends on surface modification. Specifically, I_{green}/I_{UV} has the highest value for samples from pure OD, and I_{green}/I_{UV} decreases for samples from TOA/OD and TOPO/OD. We note that since ZnO nanoparticles are dispersed in hexane, it is difficult to ensure whether the same quantity of nanoparticles is used to probe in different samples. Here, we only compared the relative intensity ratio instead of the absolute PL intensity among different samples.

Since all spherical nanoparticles have a comparable size, the quenching of green emission is most likely due to the removal of surface defects which contribute to the green luminescence. For nanoparticles synthesized from the mixture of TOA/OD in 1:10 molar ratio, it is possible that TOA removes the hydrogen from the oleic acid (deprotonation), leaving a characteristic carboxylate anionic headgroup, which then allows the oleic acid to behave as a bidentate ligand, coordinating to Zn^{2+}, and filling oxygen vacancies on or near the surface. For nanoparticles from the mixture of TOPO/OD, the bond between oxygen (O) and phosphorus (P) in TOPO is polarized. Since O is more negative in O–P bond, it tends to fill in oxygen vacancies. Thus, the introduction of TOA or TOPO can reduce the density of oxygen vacancies near the surface. The fact that we can effectively suppress the green luminescence by reducing the density of oxygen vacancies is consistent with the assumption that oxygen vacancies are the dominate defects which contribute to the green emission. Finally, we note that the quenching of green luminescence of ZnO nanoparticles by modifying surface states using chemical method has also been reported by Guo et al. [26] and Yang et al. [27]. In their work, the nanoparticles are capped by PVP. It is also important to note that other deep defects cannot be completely ignored, as it has been shown that the spectral position of the green band in ZnO nanocrystals is affected strongly by the fabrication technique [21].

Next we will discuss the plausible recombination process for the green luminescence. An oxygen vacancy has three possible charge states: the neutral oxygen vacancy (V_O^0), the singly ionized oxygen vacancy ($V_O^{\cdot}$), and the doubly ionized oxygen vacancy ($V_O^{\cdot\cdot}$). First principle calculations [30, 31] predict that the oxygen vacancies are negative-U centers. As a result, the singly ionized state is thermodynamically unstable, and the oxygen vacancies will be either in neutral or doubly charged state, depending on the Fermi level position. If as-grown ZnO nanoparticles are n-type like bulk ZnO, the neutral

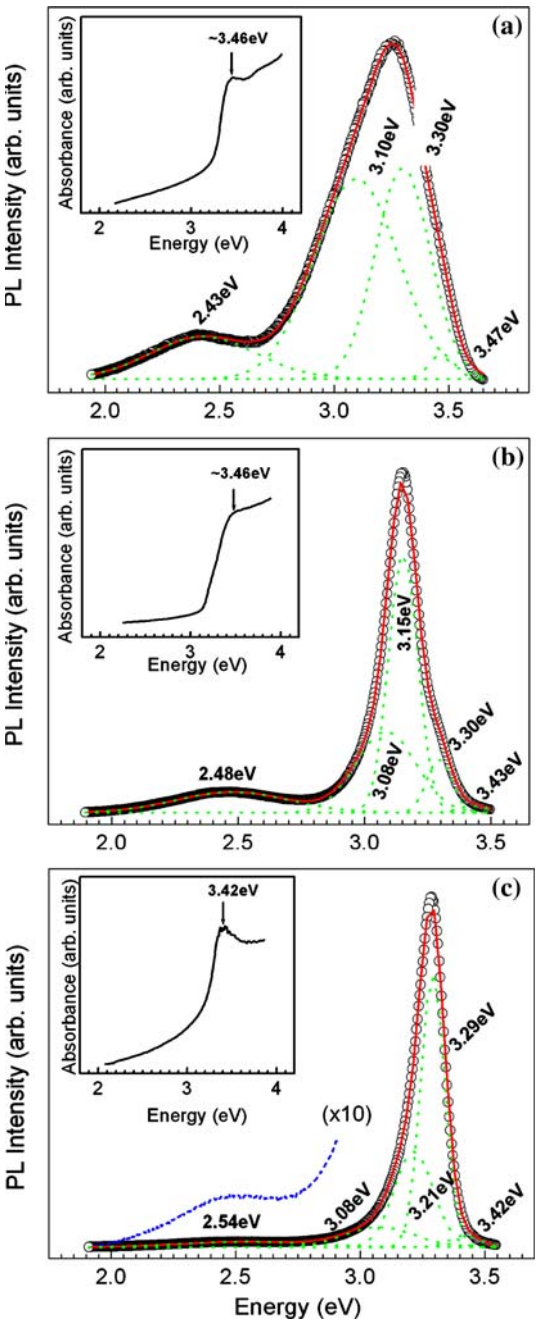

Fig. 3 (Color online) Room temperature photoluminescence (black circles) and optical absorption (inset) spectra of ZnO spherical nanoparticles prepared from (**a**) the regular solvent OD; (**b**) the mixture of TOA and OD in 1:10 molar ratio; (**c**) the mixture of TOPO and OD in 1:12 molar ratio. The PL spectra were fitted by Gaussian functions (shown as red solid line and green dotted lines)

oxygen vacancies will have the lowest formation energy, and thus will dominate.

Near the surface that ZnO exhibits a downward band bending [32], which leads to the formation of an accumulation region of electrons near the surface. It is known that the barrier height and the width of the accumulation region are related to the net positive surface charge (see below), which might be caused by donor-like surface states or adsorbed atoms [33]. Under UV illumination, electron-hole pairs will be generated, and the quasi-Fermi level of electrons and holes will shift toward conduction band and valence band, respectively. The position of the quasi-Fermi level depends on the density of the photo-generated carriers. Due to the small volume of the nanoparticles, it is possible that even at relatively low excitation the quasi-Fermi level of electrons can cross the (2+/0) level. Under such conditions, neutral vacancies will be formed near the surface, which give rise to the green luminescence via recombination with photo-generated holes, forming singly ionized vacancies: $V_O^0 + h^+ \rightarrow \ V_O + (h\nu)_{green}$. With the reduction in the concentration of the free carriers, the quasi-Fermi levels move toward mid-gap. Since singly ionized oxygen vacancies are not stable, doubly ionized vacancies will be formed to lower the total energy. Based on this recombination model, the reduction in the concentrations of oxygen vacancies will decrease the concentration of recombination centers, and thus decrease the intensity of green luminescence.

In Fig. 4 we show the measured zeta potential of nanoparticles from pure OD, the mixture of TOA/OD and the mixture of TOPO/OD. It is found that all samples have positive zeta potential, i.e. they are positively charged, which is consistent with the downward band bending, discussed above. We note that the nanoparticles from the mixture of TOA/OD and TOPO/OD have lower zeta potential than that of nanoparticles from OD. This indicates that TOA and TOPO also reduce the concentration of positively charge species on the surface which contributes to band bending. We also note that previously we reported that the addition of these chemicals might result in the reduction in the concentration of the surface oxygen vacancies [23]. However, at this point it is difficult to

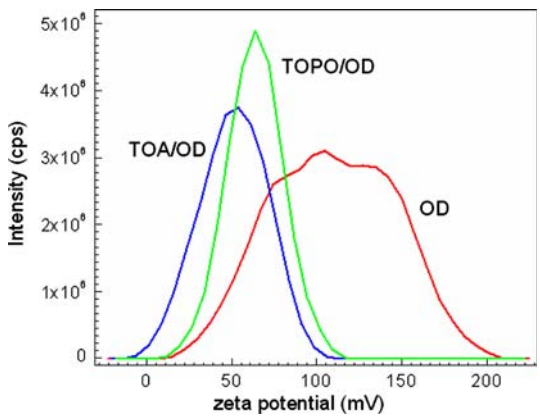

Fig. 4 Measured zeta potential of ZnO nanoparticles from (**a**) the regular solvent OD; (**b**) the mixture of TOA and OD in 1:10 molar ratio; (**c**) the mixture of TOPO and OD in 1:12 molar ratio

pinpoint an exact mechanism due to lack of detailed information about surface band bending and related surface species for ZnO (see e.g. Refs. [32, 34, 35]).

Based on the deep-level donor and hole recombination model, we estimate the size of optically active ZnO nanoparticles from the peak positions of green band. The PL was fitted by Gaussian functions, and the maximum green band energy is at ~2.44, ~2.48, and ~2.54 eV for nanoparticles from OD, TOA/OD, and TOPO/OD, respectively. We note that the UV emission of all three samples is centered at 3.42–3.47 eV, which is higher than the energy band gap of bulk ZnO. This is consistent with the small size of our spherical nanoparticles, which have a radius comparable to the Bohr radius of ZnO.

Following the assumption of Ref. [36] that the energies of the deep levels do not move appreciably with the band edges (see also Ref. [37]), we can estimate the green band energy of our spherical nanoparticles by simply adding the valence band edge shift due to the confinement [36]. Then, assuming that our nanoparticles are perfect spheres of a diameter D, the green band energy can be estimated using the following equation:

$$E_{Green}^{QD}(D) = E_{Green}^{Bulk} + \frac{2\pi^2\hbar^2}{m_h D^2}, \quad (1)$$

where the first term is the energy of the green emission in bulk ZnO ($E_{Green}^{Bulk} \approx 2.38$ eV [38–40]) and the second term is the hole quantization energy; $m_h = 0.59\ m_0$[2] is the effective mass of hole. We would like to point out that the second term does not depend on the degree of confinement, and, as expected, vanishes for very larger particles. We obtain a diameter of 6.4 nm, 5.0 nm, and 4.0 nm for $E_{Green}^{QD} = 2.44$, 2.48, and 2.54 eV, respectively. The obtained sizes are in good agreement with the TEM results (Fig. 1).

It is once more important to note that application of Eq. (1) does not have limitations on the size of spherical nanoparticles since only the quantization energy of the hole is considered. Therefore, in principal, using of Eq. (1) provides a simple and practical way to estimate size of spherical nanoparticles from optical measurements, and, moreover, this approach is applicable in all confinement regimes. We would like to point out that for the proper application of Eq. (1), samples have to be nearly monodisperse with a small size distribution. For samples of a large distribution, the green luminescence consists of contributions from particles of various sizes.

Summary

We investigated the effect of the size and surface modification on the optical properties of ZnO nanoparticles. It is found that the observed green band is most likely due to oxygen vacancies located on surfaces. By modifying surface states (achieved by introducing TOA and TOPO to the regular solvent OD), the green luminescence can effectively be quenched, which could be important for UV light emitting applications. Moreover, we used the spectral position of the green band to estimate the size of our nanoparticles, and the result shows good agreement with that obtained from TEM. It is important to note that Eq. (1) can be used for spherical nanoparticles of any size since only the quantization energy of the hole is considered. Therefore, in principal, Eq. (1) provides a straightforward and useful way to estimate the size of spherical nanoparticles from optical measurements, and is applicable in all confinement regimes.

Acknowledgements This work was supported by the MRSEC program of NSF under award number DMR-0213574. T.A. is thankful for support from the NSF GRF.

References

1. B.K. Meyer, H. Alves, D.M. Hofmann, W. Kriegseis, D. Forster, F. Bertram, J. Christen, A. Hoffmann, M. Straßburg, M. Dworzak, U. Haboeck, A.V. Rodina, Physica Status Solidi (b) **241**(2), 231 (2004)
2. O. Madelung (ed.), *Data in Science and Technology: Semiconductors* (Springer, Berlin, 1992)
3. T.-H. Moon, M.-C. Jeong, W. Lee, J.-M. Myoung, Appl. Surf. Sci. **240**(1–4), 280 (2005)
4. U. Ozgur, Y.I. Alivov, C. Liu, A. Teke, M.A. Reshchikov, S. Dogan, V. Avrutin, S.J. Cho, H. Morkoc, J. Appl. Phys. **98**(4), 41301 (2005)
5. S.J. Pearton, C.R. Abernathy, M.E. Overberg, G.T. Thaler, D.P. Norton, N. Theodoropoulou, A.F. Hebard, Y.D. Park, F. Ren, J. Kim, L.A. Boatner, J. Appl. Phys. **93**(1), 1 (2003)
6. A. Tsukazaki, A. Ohtomo, T. Onuma, M. Ohtani, T. Makino, M. Sumiya, K. Ohtani, S.F. Chichibu, S. Fuke, Y. Segawa , H. Ohno, H. Koinuma, M. Kawasaki. Nat. Mater. **4**(1) 42 (2005)
7. A.P. Alivisatos, Science **271**, 933 (1996)
8. Z. Fan, J.G. Lu. J. Nanosci. Nanotechnol. **5**(10), 1561 (2005)
9. F. Wang, Z. Ye, D. Ma, L. Zhu, F. Zhuge . J. Cryst. Growth **274**(3–4), 447 (2005)
10. G.-C. Yi, C. Wang, W.I. Park, Semicond. Sci. Technol. **20**(4), 22 (2005)
11. D.-F. Zhang, L.-D. Sun, J.-L. Yin, C.-H. Yan, R.-M. Wang, J. Phys. Chem. B **109**(18), 8786 (2005)
12. C. Jagadish, S. Pearton (eds.), *ZnO bulk, thin films, and nanostructures* (Elsevier, 2006)
13. H.S. Kang, J.S. Kang, J.W. Kim, S.Y. Lee, J. Appl. Phys. **95**(3), 1246 (2004)
14. S.A. Studenikin, N. Golego, M. Cocivera, J. Appl. Phys. **84**(4), 2287 (1998)
15. K. Vanheusden, C.H. Seager, W.L. Warren, D.R. Tallant, J.A. Voigt, Appl. Phys. Lett. **68**(3), 403 (1996)
16. L. Wu, Y. Wu, X. Pan, F. Kong, Opt. Mater. **28**(4), 418 (2006)
17. S.B. Zhang, S.H. Wei, A. Zunger, Phys. Rev. B **63**(7), 075205 (2001)
18. F. Tuomisto, K. Saarinen, D.C. Look, G.C. Farlow, Phys. Rev. B (Condens. Matter Mater. Phys.) **72**(8), 085206 (2005)

19. D.C. Reynolds, D.C. Look, B. Jogai, J. Appl. Phys. **89**(11), 6189 (2001)
20. B. Guo, Z.R. Qiu, K.S. Wong, Appl. Phys. Lett. **82**(14), 2290 (2003)
21. D. Li, Y.H. Leung, A.B. Djurisic, Z.T. Liu, M.H. Xie, S.L. Shi, S.J. Xu, W.K. Chan, Appl. Phys. Lett. **85**(9), 1601 (2004)
22. M. Yin, Y. Gu, I.L. Kuskovsky, T. Andelman, Y. Zhu, G.F. Neumark, S. O'Brien, J. Am. Chem. Soc. **126**, 6206 (2004)
23. T. Andelman, Y. Gong, M. Polking, M. Yin, I. Kuskovsky, G. Neumark, S. O'Brien, J. Phys. Chem. B **109**(30), 14314 (2005)
24. S. Sakohara, M. Ishida, M.A. Anderson, J. Phys. Chem. B **102**(50), 10169 (1998)
25. G. Lin, Y. Shihe, Y. Chunlei, Y. Ping, W. Jiannong, G. Weikun, G.K.L. Wong, Appl. Phys. Lett. **76**(20), 2901 (2000)
26. L. Guo, S. Yang, C. Yang, P. Yu, J. Wang, W. Ge, J.K.L. Wong, Appl. Phys. Lett. **76**, 2901 (2000)
27. M.H. Huang, S. Mao, H. Feick, H. Yan, Y. Wu, H. Kind, E.Weber, R. Russo, P. Yang, Science **292**(5523), 1897 (2001)
28. Y. Harada, S. Hashimoto, Phys. Rev. B **68**(4), 45421 (2003)
29. I. Shalish, H. Temkin, V. Narayanamurti, Phys. Rev. B **69**(24), 245401 (2004)
30. P. Erhart, K. Albe, A. Klein, Phys. Rev. B **73**(20), 205203 (2006)
31. A. Janotti, C.G. Van de Walle, Appl. Phys. Lett. **87**(12), 122102 (2005)
32. B.J. Coppa, C.C. Fulton, S.M. Kiesel, R.F. Davis, C. Pandariath, J.E. Burnette, R.J. Nemanich, D.J. Smith, J. Appl. Phys. **97**, 103517/13 (2005)
33. W. Monch, *Semiconductor Surfaces and Interfaces*, 3rd edn. ed. by G. Ertl, R. Gomer, H. Luth, D.I. Mills. (Springer, Berlin, New York, 2001)
34. S.A. Chevtchenko, J.C. Moore, U. Ozuger, X. Gu, A.A. Baski, H. Morkoc, B. Nemeth, J.E. Nause, Appl. Phys. Lett. **89**, (2006)
35. S.J. Cho, S. Dogan, S. Sabuktagin, M.A. Reshchikov, D.K. Johnstone, H. Morkoc, Appl. Phys. Lett. **84**(16), 3070 (2004)
36. Y. Gu, I.L. Kuskovsky, M. Yin, S. O'Brien, G.F. Neumark, Appl. Phys. Lett. **85**(17), 3833 (2004)
37. A.L. Efros, M. Rosen. Ann. Rev. Mater. Sci. **30**(1), 475 (2000)
38. D. Banerjee, J.Y. Lao, D.Z. Wang, J.Y. Huang, Z.F. Ren, D. Steeves, B. Kimball, M. Sennett, Appl. Phys. Lett. **83**(10), 2061 (2003)
39. B. Lin, Z. Fu, Y. Jia, Appl. Phys. Lett. **79**(7), 943 (2003)
40. X. Liu, X. Wu, H. Cao, R.P.H. Chang, J. Appl. Phys. **95**(6), 3141 (2004)